Investigation of toughness of ultra high performance fibre reinforced concrete (UHPFRC) beam under impact loading

L. Mao[1]*, S.J. Barnett[2]

[1]Department of Aeronautical and Automotive Engineering, Loughborough University, Epinal Way, Loughborough, LE11 3TU, UK

[2]School of Civil Engineering and Surveying, University of Portsmouth, Winston Churchill Avenue, Portsmouth, PO1 2UP, UK

* Corresponding author l.mao@lboro.ac.uk

Abstract:

This paper provides a systematic study about toughness of ultra high performance fibre reinforced concrete (UHPFRC) in order to better understand the UHPFRC resistance under impact loading condition. UHPFRC beams containing various fibre volumes are tested under impact load at different strain rate. From the test results, the relationship between UHPFRC toughness and strain rate can be determined. Moreover, a numerical model of UHPFRC beam under impact load is developed and its performance is verified using test data. With developed UHPFRC model, the evolution of UHPFRC toughness can be better investigated.

Keywords:

UHPFRC, toughness, impact load, numerical simulation, strain rate

1 Introduction:

As ultra high performance fibre reinforced concrete (UHPFRC) material has significant higher strength than the normal strength concrete, it is more commonly used in civil engineering field, especially applications associated with high strain rate loadings. Therefore, in order to maximize the advantages of UHPFRC, its properties and performance under these loading conditions have received much attention in the last few decades.

Habel et al. (2006) studied the evolution of UHPFRC properties, including strength, stiffness, related to hydration. Isaacs et al.(2009) designed novel techniques to perform material characterization tests on UHPFRC, including compression and tension tests. With these tests, the compressive and tensile behaviours of UHPFRC could be investigated. Kang et al.(2010), Kim et al.(2011), and Park et al.(2012) performed several tests to study the tensile behaviour of UHPFRC with various fibre volumes. Moreover, blast tests were carried out by Gupta et al.(2007), Ngo et al.(2007), Barnett, S.J.(2008), Yi et al.(2012), Mao et al. (2014, 2015) to investigate performance of UHPFRC, including deflection and crack pattern, under blast loading.

According to previous studies, due to its high strength, UHPFRC can perform better than conventional concrete material under high strain rate loadings. Moreover, similar to normal strength concrete material, UHPFRC properties, such as compressive strength, tensile strength, and elastic modulus, will be increased with strain rate, but dynamic increase factor (DIF) values of UHPFRC at various strain rates are different to that from normal strength concrete, which can be found in Millard et al. 2010, where the dynamic increase factors of tensile and shear strengths at various strain rate values, with a series of tensile and shear tests on UHPFRC specimen.

However, as another important parameter, toughness can represent the energy absorbing ability of the material, and can be used to determine the resistance to the fracture under loading condition, but investigation of toughness has received less attention in the past few years, especially at high rate loading conditions. Barnett (2008) performed tests on UHPFRC beam with drop hammer method, and indicated the beam toughness would change with strain rate. Some other investigations have also been performed to UHPFRC specimen to clarify the relationship between UHPFRC toughness and strain rate (Cotsovos, 2010, Mechtcherine et al. 2011, Bragov et al. 2013), but the results are still inconclusive and even contradictory. Therefore, it is necessary to perform a systematic investigation to UHPFRC specimen, so that the evolution of UHPFRC toughness with strain rate can be better understood.

This paper presents a systematic study to investigate toughness of UHPFRC beam containing various fibre volumes at different strain rates. In the tests, drop hammer method is used, that is, hammer is released at different heights to achieve various strain rate values, and fibreboards are employed to attenuate the hammer load. As the load is measured at beam supports, it also contain information related to beam vibration, this effect will be investigated in this study by analysing frequency spectrum of measured support load, and will be removed with designed filter. With processed support load and beam deflection, the toughness value could be obtained and relationship between UHPFRC toughness and strain rate was determined. Moreover, numerical analysis is performed in the study to obtain UHPFRC toughness at wider range of strain rate. The stress-strain curve of numerical model is configured to match design stress-strain relationship of UHPFRC, and performance of developed models is verified by comparing force-deflection relationship with tested UHPFRC

65 beams. With both experimental tests and numerical analysis, the evolution of UHPFRC
66 toughness with strain rate can be better understood.

67 2 Experimental study of UHPFRC beam toughness with strain rate

68 In this section, the mix proportions of tested UHPFRC beams are described, and drop
69 hammer tests is applied to UHPFRC beams. From tests, support loads and UHPFRC
70 deflection can be obtained to generate UHPFRC toughness, it should be mentioned that
71 information contained in measured support load is further investigated, and design filter
72 will be used to remove beam vibration effect from measured support load. With test data,
73 UHPFRC beam toughness at various strain rates will be investigated, and relationship
74 between UHPFRC beam toughness and strain rate can be better understood.

75 2.1 Description of UHPFRC beam

76 In the study, the tested UHPFRC beam is manufactured at University of Liverpool, they are
77 cast horizontally and compacted using a vibrating table. Beams are produced in batches of three
78 panels. Cube specimens are also manufactured from each batch in order to measure compressive
79 strength of the concrete and check consistency of the results between batches. After 24 hours, all
80 specimens are removed from the moulds and transferred to a hot water curing tank set at 90 °C
81 where they remain until they were 7 days old. Following this hot curing treatment, there is very
82 little further change in the compressive strength of the concrete. Optimized packing density of
83 UHPFRC beam is achieved using 10% fine silica fume with typical particle size of 100-500nm,
84 and 35% ground granulated blast furnace slag (GGBS) is also employed to replace cement in
85 the concrete to increase its workability. Table 1 lists the detailed mix proportions of UHPFRC
86 beam used in the tests.

87 Table 1 Mix proportions of UHPFRC beam

Cementitious component (kg/m^3)				Aggregate Sand (kg/m^3)	Water-binder ratio	Structuro 1180 superplasticiser
Cement	GGBS	Silica fume	Whole			
657	418	119	1194	1051	0.17	40

88

89 Moreover, short steel fibres are added to UHPFRC beam to enhance its flexural strength.
90 Three kinds of steel fibre combinations are selected in the study, including 2% short steel
91 fibres (13mm in length) by volume, 6% short steel fibres (13mm in length) by volume, and 6%
92 hybrid steel fibres (3% short fibre of 13mm long, and 3% long fibre of 25mm long) by
93 volume. The use of hybrid fibre is to investigate the enhanced post-cracking performance of
94 UHPFRC beam with combination of several steel fibre types.

95 In the manufacturing process, the elevated temperature curing technique is used to the
96 UHPFRC beam, the tested specimens are cured under damp Hessian for 24 hours, then
97 these specimens are conditioned at 90℃ in hot water tank for six days.

98 The dimension of tested UHPFRC beam is 350mm×100mm×50mm. In the tests, the beam is
99 simply supported, giving effective beam span of 300mm, and is rotated through 90° so that
100 its top and bottom surfaces are smooth surfaces.

101 2.2 Drop hammer test

102 In the study, the drop hammer technique is used to investigate UHPFRC beam behaviour at
103 various strain rates. The weight of drop hammer is 23.3kg and its maximum release height is

2m. Moreover, fibreboard with 10mm thickness is employed in the test. Therefore, strain rate could be adjusted by using different layers of fibreboards and hammer release heights.

It should be noted that as the applied load from drop hammer can not be measured directly, the support loads is measured with load cells beneath the roller supports, which is depicted in Figure 1. It can be seen from figure that load cells are located on a 50mm thick steel base, which is located on a 10mm layer of fibreboard.

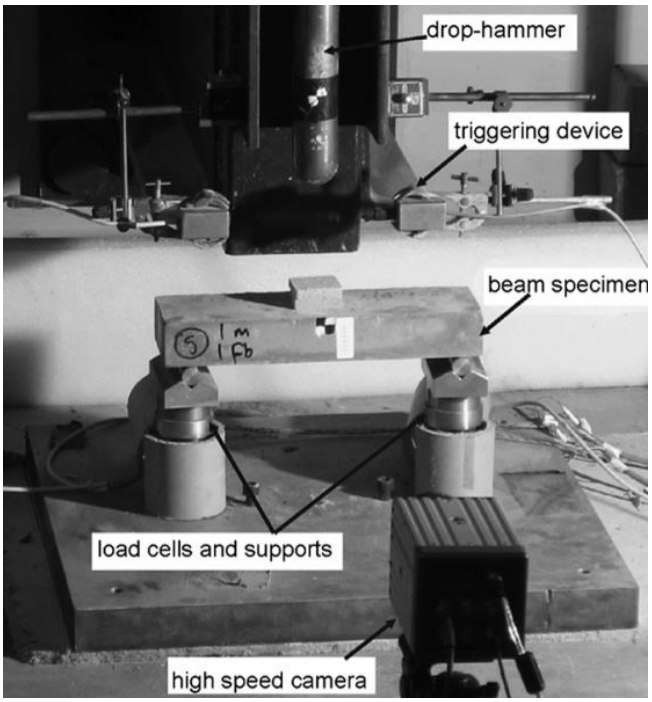

Figure 1 Drop hammer test

Moreover, deflection of UHPFRC beam (marked position in Figure 1) is measured in the tests with high speed camera placed in front of UHPFRC beam, and signal filtering is applied to reduce the noise level in measured deflections.

116 In this study, the strain rate is calculated using bending beam theory, which has been
117 adopted for the strain rate calculation in previous studies (Cotsovos, 2010, Millard et al.
118 2010), the measured deflection is used to calculate the maximum strain in the beam, and
119 then maximum strain rate is obtained by differentiating strain with respect of time.

120 With the measured support load and beam deflection, the load-deflection curve can be
121 formed, and beam toughness can be obtained by calculating area below the load-deflection
122 curve. By adjusting hammer release height and layers of fibreboard, various strain rates can
123 be obtained and its effect on UHPFRC beam toughness could be evaluated.

124 2.3 Results from drop hammer tests

125 In the tests, UHPFRC beams with 2%, 6% and 6% hybrid fibre volumes are used to study the
126 strain rate effect on UHPFRC toughness. As mentioned above, various hammer release
127 heights and layers of fibreboard are used to get different strain rates.

128 2.3.1 Investigation of measured support loads from tests

129 As above description, the loads measured from load cells are employed to generate load-
130 deflection curve, and it is verified from the previous studies that this measured load could
131 match well with the loads from the hammer, although more ‘noises’ appear in measured
132 load from load cells [Millard et al. 2010]. Figure 2 depicts two measured loads from load
133 cells, which were obtained from UHPFRC beams with 2% and 6% fibre volumes, with impact
134 load generated by releasing hammer at 2m, and 2 layers of 10mm thick fibreboards on the
135 top of beam. It can be seen that in both cases, the measured support load contains many
136 'noisy' spurs. Therefore, before using these measured loads for the analysis, these spurs
137 should be removed from the load measurements.

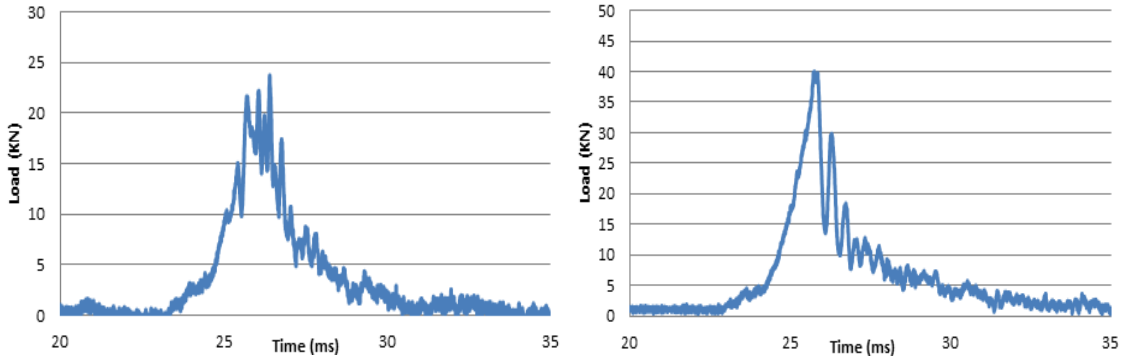

Figure 2 Measured supports loads from beam with 2% fibre volume (left) and 6% fibre volume (right)

In this analysis, the high-pass Butterworth signal filter was designed and applied to remove these noises, with cut-off frequency of 500Hz. The curt-off frequency is selected based on the natural frequencies of the UHPFRC beams (which is described in section 3.2), so that information from the UHPFRC beams will not be removed with the filter. Figure 3 depicts the original measured support load and processed support load after applying filter, it can be seen that the spurs due to beam vibration can be removed effectively, and the support load can better represent the impact load from drop hammer.

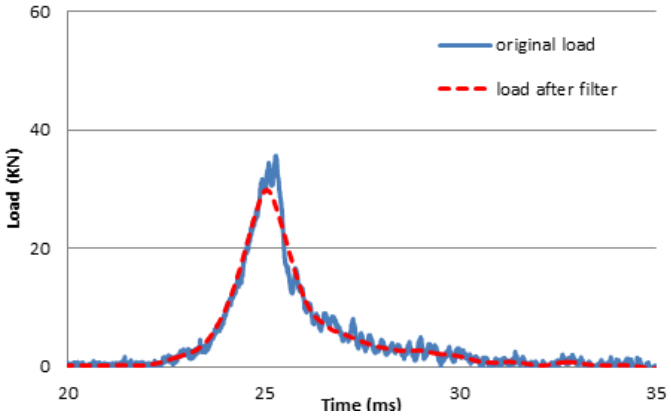

Figure 3 Comparison of support loads before and after applying filter

2.3.2 Strain rate effect on toughness of UHPFRC beam with 2% fibre volume

For UHPFRC beams with 2% fibre volume, drop hammer is released from 0.5m, 1m and 2m to give different strain rates, and 2 layers of 10mm thick fibreboards are placed on the top of beam to attenuate the applied load. For each case, support load after applying designed filter and beam deflection are used to generate load-deflection curve, which is depicted in Figure 4. It should be mentioned that for illustration purpose, only one load-deflection from each case curve is shown in the figure, although several tests are repeated for each case.

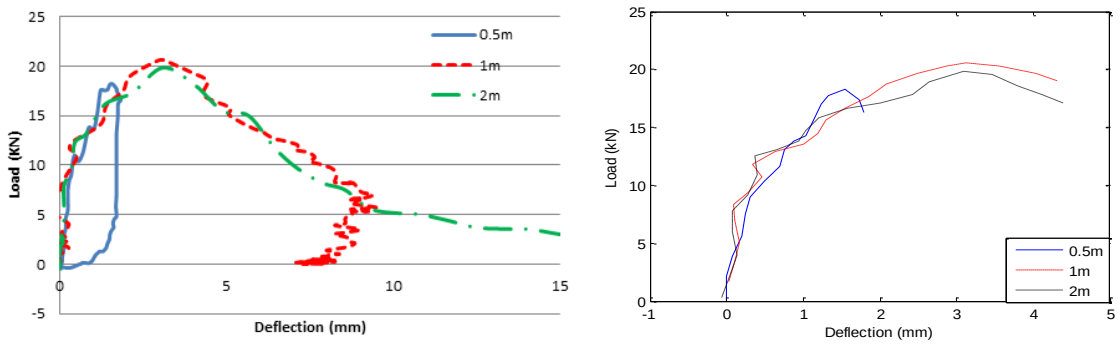

(a) Whole load-deflection curve (b) Load-deflection curve for toughness study

Figure 4 Load-deflection curves of UHPFRC beams with 2% fibre volume at various release heights

From Fig.4(a) it can be seen that hammer release height of 0.5m only give small deflection of the UHPFRC specimen and strain hardening behaviour can not be observed. With increased hammer release height, serious cracks in the specimen are found and strain hardening is observed in the load-deflection curve. Moreover, the toughness of UHPFRC specimen is studied and shown in Fig.4(b), the toughness does not show clearly toughness change trend within the studied strain rate range. The possible reason is that as fibre is randomly oriented and distributed in the specimen, which could affect flexural strength of UHPFRC specimen (Stephanie et al. 2010), thus the increase trend in specimen toughness may be masked by this random effect, this will be further investigated in the later part using numerical study.

To further study the beam damages due to the impact hammer from various releasing heights, the beam mid-span deflections from different hammer releasing heights are depicted in Fig.5. It can be seen that 0.5m hammer releasing height does not cause significant damage to the specimen, as the specimen vibrates and return to the original position after the impact load, while permanent deformation can be found under impact load with 1m hammer release height, indicating the existence of severe damage to the specimen, with further increase of hammer releasing height to 2m, the specimen will be completely broken into 2 parts. It should be mentioned that in the UHPFRC specimen with 2% fibre volume, the impact hammer will cause the bending failure to the beam with the cracks at/near the beam mid-span.

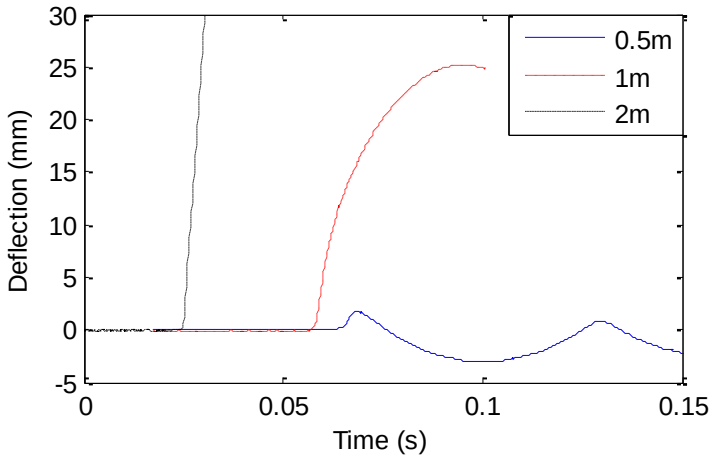

Figure 5 Mid-span deformation of UHPFRC beam with 2% fibre volume under various impact hammer releasing heights

Moreover, more layers of fibreboards are also used in the tests so that wider range of strain rates could be obtained. Two and six layers of fibreboards are employed for UHPFRC beams with 2% fibre volume, and hammer is released at 2m height, corresponding load-deflection

curves are depicted in Figure 6. For each case, three load-deflection curves are shown in Figure 5 to better illustrate the change of UHPFRC toughness.

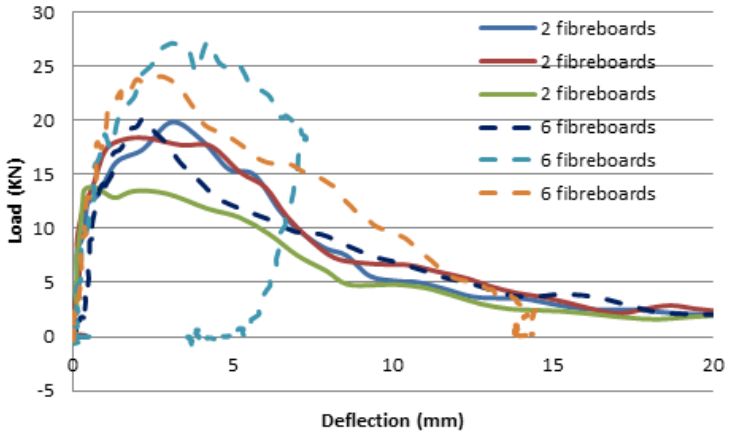

(a) Whole load-deflection curve

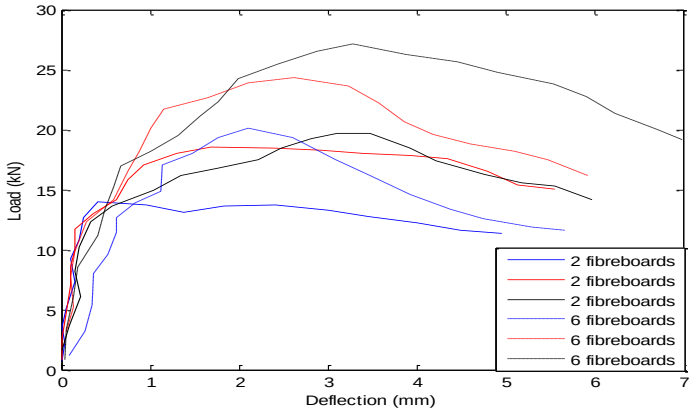

(b) Load-deflection curve for toughness study

Figure 6 Load-deflection curves of UHPFRC beams with 2% fibre volume at various layers of fibreboards

From Figure 6, with increased layers of fibreboards, which gives smaller strain rate values, the reduction of beam toughness can not be observed clearly, in some cases the UHPFRC beam with 6 fibreboards even give higher toughness, this can be found in Fig.6(b). Moreover, with 6 layers of fibreboards, most UHPFRC specimens still have complete fracture after the

197 impact load. It should be noted that the UHPFRC specimen with the same fibreboards give
198 different load-deflection curve, this is caused by the effect of random fibre orientation and
199 distribution, which may be the reason that the increase trend of specimen toughness with
200 strain rate can not be observed.

201 Figure 7 depicts the time-history of impact load to the UHPFRC specimen with different
202 number of fibreboards. It can be observed that with increase fibreboards (causing smaller
203 strain rate), impact load with higher amplitude can be generated. Moreover, more
204 fibreboards can give longer impact load duration and smaller loading rate to the UHPFRC
205 specimen.

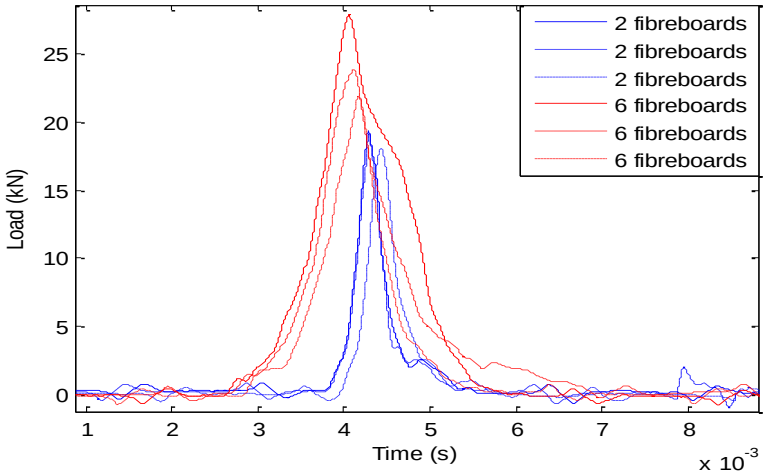

206

207 Figure 7 Time-history of impact load to 2% fibre volume UHPFRC specimen with different
208 fibreboards

209 Moreover, in order to better illustrate the effect of strain rate on UHPFRC toughness, the
210 strain rate and toughness (which is defined as the area below load-deflection curve) are
211 calculated from each case, and toughness-strain rate relationship can be evaluated.

With this method, strain rate is calculated and its effect on toughness can be evaluated by studying the relationship between the UHPFRC beam toughness and strain rate, which is depicted in Figure 8, it should be noted that the exponential function is fitted to match the test data points.

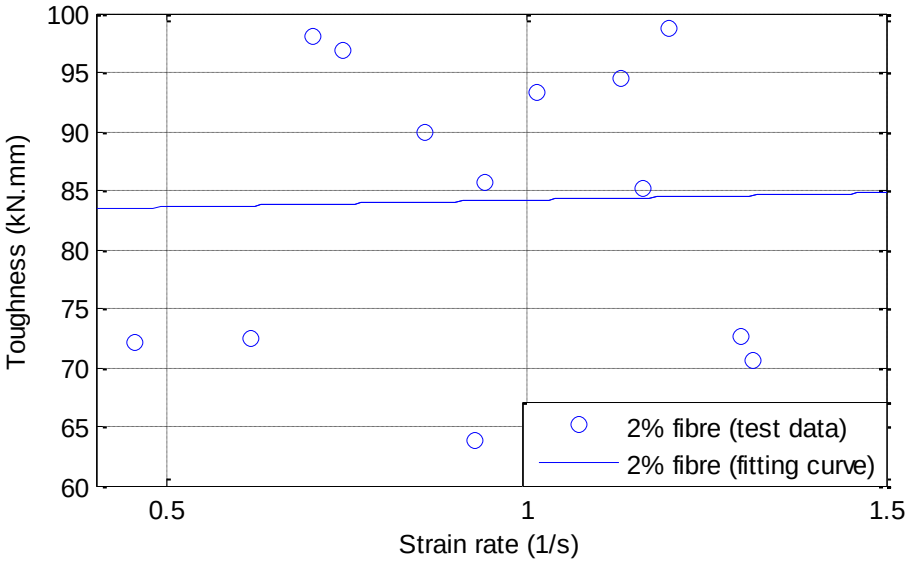

Figure 8 Relationship of strain rate and absorbed energy of UHPFRC beams with 2% fibre volume

It can be seen from above figure that the strain rate increase trend cannot be found clearly with strain rate. Moreover, it should be noted that the curve starts with the strain rate of $0.4s^{-1}$, the reason is that below this value, the beam only experience small deflection, and strain hardening can not be observed, thus the toughness is not included in the analysis.

As increase of UHPFRC specimen toughness with strain rate can not be observed with beam having 2% fibre volume, the UHPFRC beam containing higher fibre volume will be employed to obtain the toughness change with strain rate.

2.3.3 Strain rate effect on UHPFRC beam with 6% fibre volume

Similar to UHPFRC beam with 2% fibre volume, drop hammer is released at various heights to get different strain rates, and load-deflection curves are obtained. 0.5m, 1m, 1.5m and 2m release heights are used and corresponding load-deflection curves are shown in Figure 9. It should be mentioned that filter is applied to measured support loads to remove component from beam vibration. Only one curve is depicted in each release height in order to better express the change of beam toughness. 2 layers of 10mm thick fibreboards are used in these cases to attenuate the hammer load.

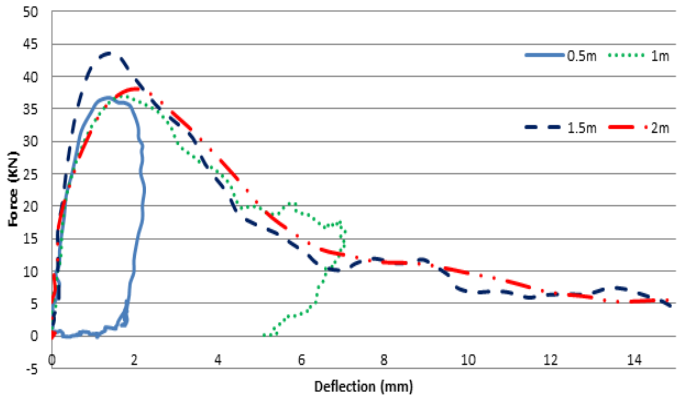

(a) Whole load-deflection curve

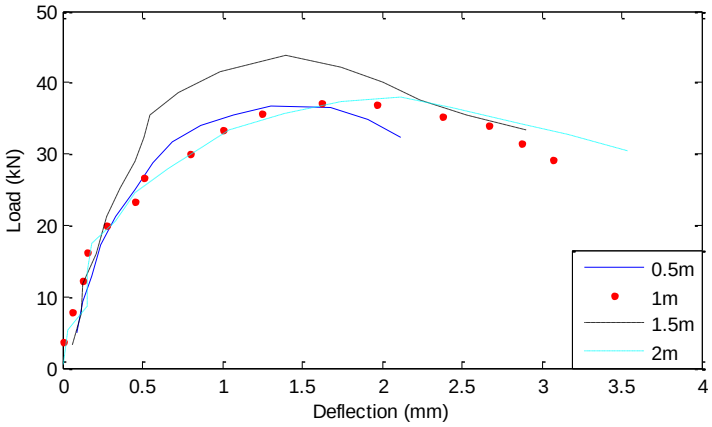

(b) Load-deflection curve for toughness study

Figure 9 Load-deflection curves of UHPFRC beams with 6% fibre volume at various release heights

From above Figure, it can be observed that the beam toughness increased with hammer release height from 0.5m to 1.5m, and increase trend at 2m hammer release height can not be seen due to the random effect of fibre orientation and distribution, which is similar to that in specimen with 2% fibre volume.

Furthermore, the mid-span deformation of specimen under various hammer releasing heights are depicted in Figure 10, and the specimen after the impact hammer is shown in Figure 11 to study the damage of UHPFRC specimen with 6% fibre volume due to the impact hammer.

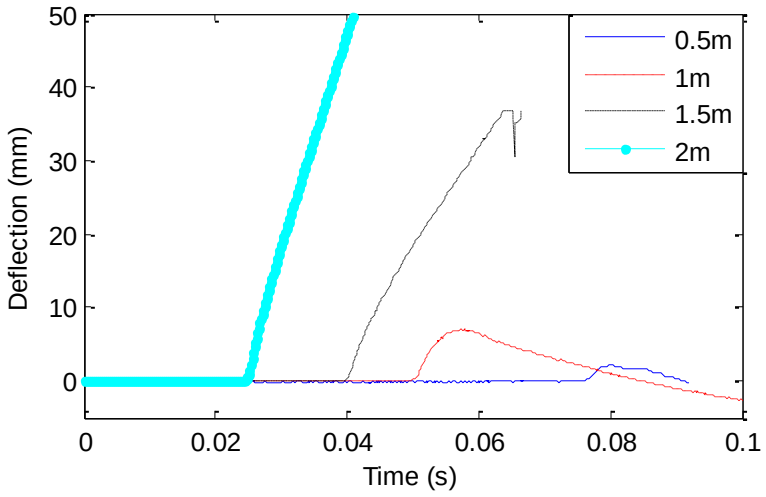

Figure 10 Mid-span deformation of UHPFRC beam with 6% fibre volume under various impact hammer releasing heights

Figure 11 UHPFRC specimen with 6% fibre volume after the impact test

It can be seen from Figure 10 that compared to the mid-span deformation of UHPFRC specimen with 2% fibre volume (shown in Figure 5), UHPFRC specimen with 6% fibre volume does not show severe damage under 1m high impact hammer, since permanent deformation is not observed in this case, this indicate the effect of fibre volume in improve the UHPFRC resistance to the impact load. With further increase hammer release height, permanent deformation and severe damage can be found in UHPFRC specimen with impact load of 1.5m release height, and under 2m high impact hammer, the UHPFRC specimen is broken into 2 parts completely. Similar to UHPFRC specimen with 2% fibre volume, UHPFRC specimen with 6% fibre volume shows the bending failure mode under the impact loading, and the crack is observed at/near the mid-span of specimen, which is shown in Figure 11.

Moreover, the effect of fibreboard number on load-deflection curve is also investigated. Two and five layers of fibreboards are used in the tests with 2m release height of drop hammer to get various strain rate values. Figure 12 shows the load-deflection curves for two and five layers of fibreboards cases.

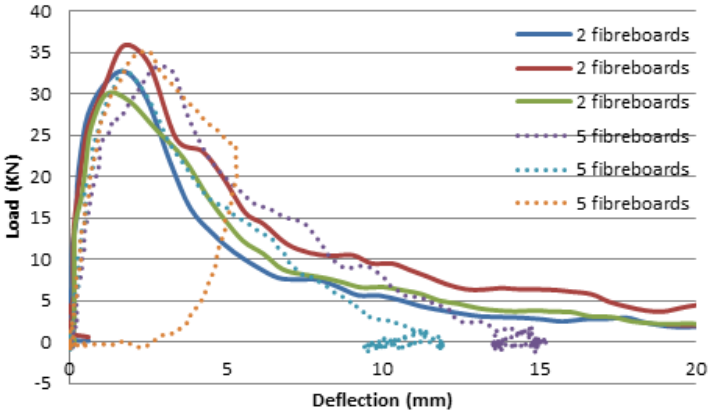

(a) Whole load-deflection curve

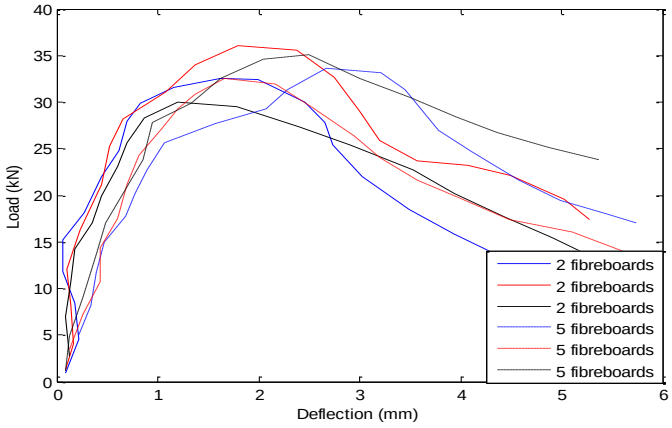

(b) Load-deflection curve for toughness study

Figure 12 Load-deflection curves of UHPFRC beams with 6% fibre volume at various layers of fibreboards

It can be seen from above figure that with this method, the clearly increase trend of specimen toughness with strain rate cannot be observed. It should be noted that the results in UHPFRC specimen with 2% fibre volume (increased specimen toughness with reduced strain rate) are not found in specimen with higher fibre volume.

Figure 13 shows the time-history of impact load to the 6% fibre volume UHPFRC specimen with different number of fibreboards. Similar to UHPFRC specimen with 2% fibre volume, using more fibreboards can clearly increase the impact load duration, which can effectively

provide the lower impact loading rate. This is consistent to the results from UHPFRC specimen with 2% fibre volume.

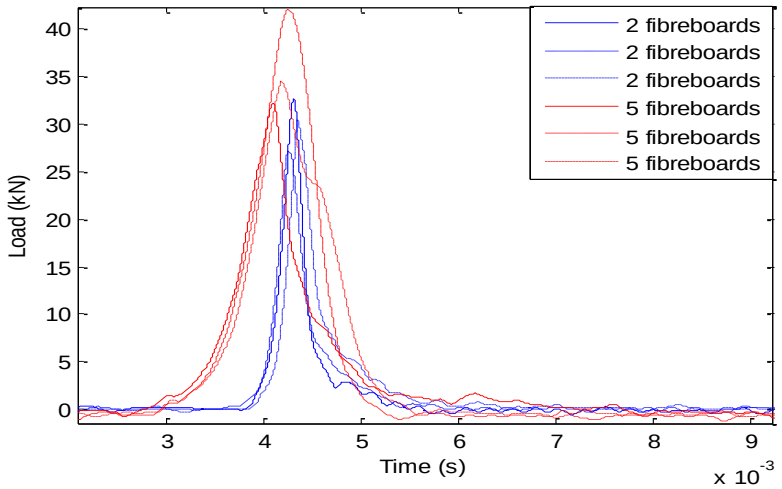

Figure 13 Time-history of impact load to 6% fibre volume UHPFRC specimen with different fibreboards

Furthermore, strain rate value is calculated in each test with bending beam theory and its effect on UHPFRC beam toughness is evaluated and depicted in Figure 14, and a curve is fitted to match the data points.

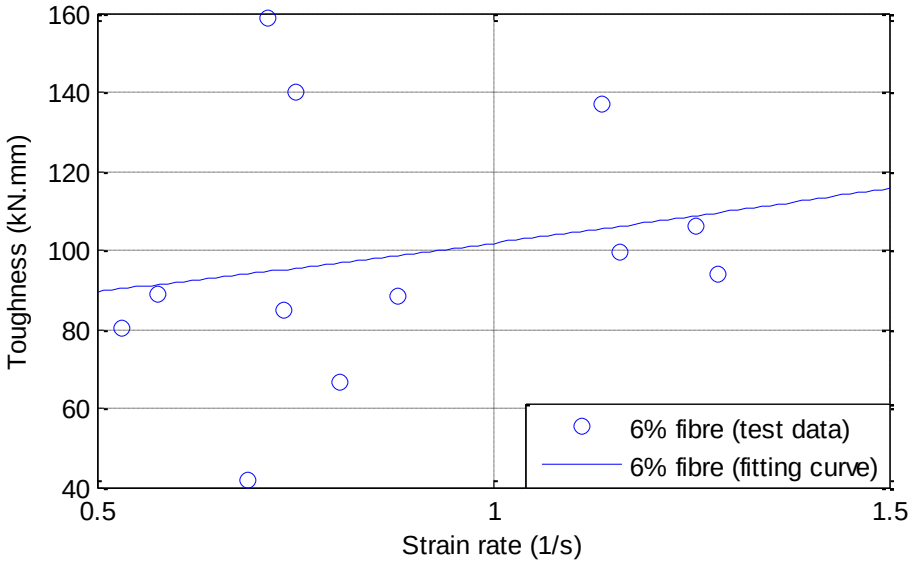

287

288 Figure 14 Relationship of strain rate and absorbed energy of UHPFRC beams with 6% fibre volume

289 From above figure, it can be observed that in the investigated range of strain rate, beam
290 toughness will increase with strain rate, but this trend is not clearly. It should be mentioned
291 that with increase of fibre volume, the beam resistance to impact loading will be increased
292 accordingly, this can be found with the starting strain rate in Fig.9, which is about $0.6s^{-1}$, as
293 below this value the beam experiences small deflection and can not express strain
294 hardening behaviour. Therefore, the increase of fibre volume can improve UHPFRC
295 performance and reduce the random effect due to fibre orientation and distribution.

296 2.3.4 Strain rate effect on UHPFRC beam with 6% hybrid fibre volume

297 In order to study the effect of fibre combination on UHPFRC behaviour, UHPFRC beams with
298 6% hybrid fibre volume are tested, and results are compared to those from beams with 6%
299 fibre volume. In the tests, two and four layers of fibreboards are employed to get different
300 strain rate values, and load-deflection curves from those tests are obtained and depicted in

Figure 15. It should be mentioned that the release height of drop hammer is fixed to 2m for UHPFRC beam with 6% hybrid fibre volume.

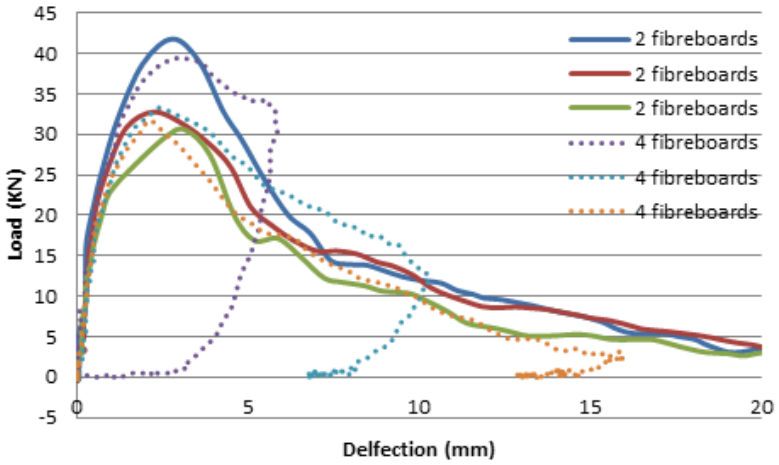

(a) Whole load-deflection curve

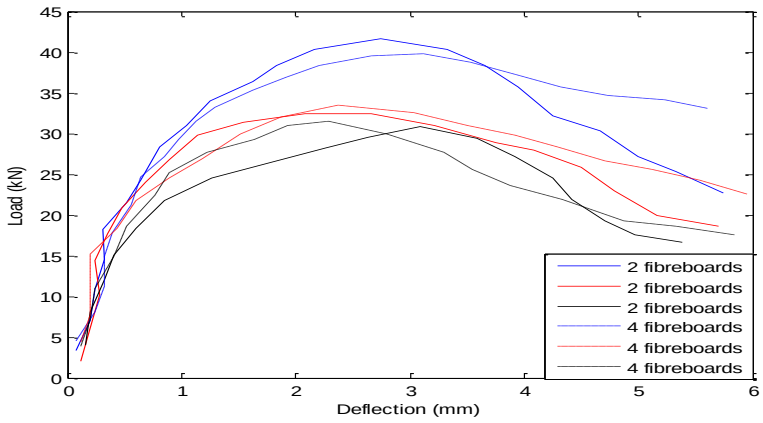

(b) Load-deflection curve for toughness study

Figure 15 Load-deflection curves of UHPFRC beams with 6% hybrid fibre volume at various layers of fibreboards

From above results, the increase of strain rate using reduced number of fibreboards can not give higher specimen toughness, which is similar to results in UHPFRC specimen with 6% fibre volume. Moreover, similar to UHPFRC beams with 6% fibre volume, all the tested

beams with 4 layers of fibreboards can survive the impact loading without complete fracture.

In order to better illustrate the effects of fibre combination, the beam toughness-strain rate curves for UHPFRC beams with 6% fibre and 6% hybrid fibre volumes are compared and depicted in Figure 16. It can be seen that the use of fibre combination in this study can increase the UHPFRC specimen toughness, but this effect is not clearly.

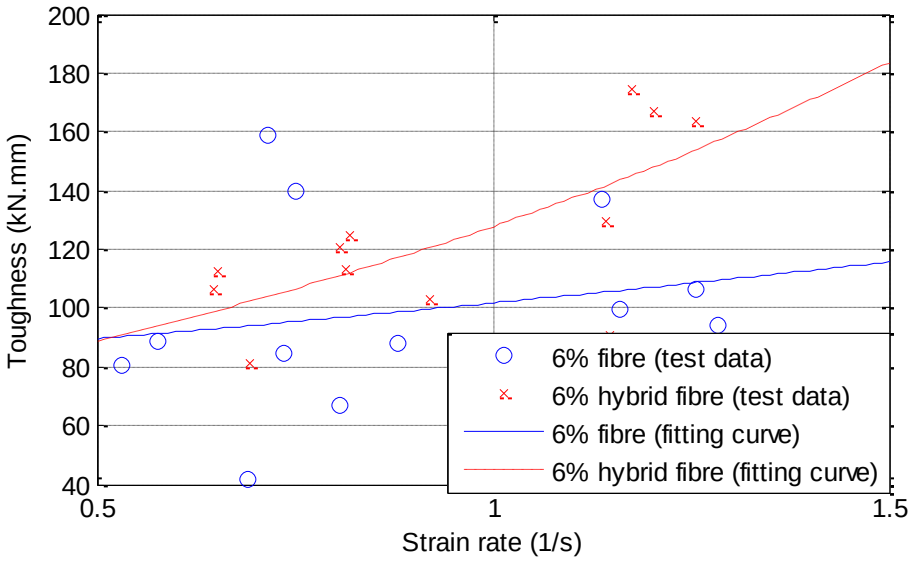

Figure 16 Comparison of UHPFRC absorbed energy-strain rates curves from UHPFRC beams with 6% fibre volume and 6% hybrid fibre volume

From above results, it can be concluded that the increase of fibre volume can improve the UHPFRC specimen resistance effectively, UHPFRC specimen with 2% fibre volume experiences complete fracture at strain rate of $0.4s^{-1}$, while UHPFRC specimen with 6% fibre volume is broken into two parts at $0.6s^{-1}$ stain rate. Moreover, with UHPFRC specimen containing higher fibre volume, the increase of specimen toughness with strain

rate can be observed, this indicate effect due to fibre random orientation and distribution can be reduced with increase of fibre volume. However, the use of fibre combination (different fibre lengths in this study) can increase the UHPFRC toughness, especially at high strain rate range.

3. Numerical study of UHPFRC beam toughness with strain rate

In the above section, experimental study is used to investigate the flexural toughness of UHPFRC beam by measuring support load and beam deflection. In the tests, several methods, including using different fibreboard layers, releasing hammer from various heights, are employed to get strain rates from $0.2s^{-1}$ to $1.5s^{-1}$.

However, in the tests, the fibre orientation and distribution was not measured in UHPFRC beams, which may prevent the clearly relationship between UHPFRC toughness and strain rate, as the random fibre orientation and distribution may cause variation in the UHPFRC behaviour [Stephanie, et al. 2010, Mao, et al. 2015]. Therefore, in order to further investigate the evolution of beam toughness with strain rate, numerical method is employed herein to remove the influence due to random fibre orientation and distribution.

3.1 Development of numerical model

In this study, the concrete damage model, also called K&C model, in LS-DYNA is used to simulate behaviour of UHPFRC beam. In K&C model, three independent strength surfaces, including initial yield, maximum failure, and residual surfaces, are defined, strain hardening and softening behaviours can also be expressed with strength surfaces interpolated between three defined strength surfaces, and strain rate effect can be expressed by defining strength enhancements in compression and tension separately (Malvar et al. 1997, 2000, Tu and Lu, 2009).

The capability of K&C model in simulating concrete materials under various loading conditions has already been investigated by previous studies (Tanapornraweekit et al. 2007, Odeh, 2008). Results demonstrated that the behaviour of normal strength concrete can be modelled with good quality with K&C model.

An important reason of using K&C model is that it contains an automatic model generation method. With this method, only concrete compressive strength is required, and all other concrete properties can be calculated automatically. This makes K&C model suitable in this study, as only limited UHPFRC properties are measured from tests (Magallanes et al. 2010).

However, it should be mentioned that the automatic model parameter generation method is developed based on test data from normal strength concrete (with compressive strength of about 35MPa), when it is applied to UHPFRC, even with input UHPFRC compressive strength (about 170MPa), the behaviour of developed model may not express actual UHPFRC performance, especially improved strain hardening and softening behaviours of UHPFRC. Therefore, after generating model parameters automatically, further modifications should be performed to the generated parameters, especially those controlling strain hardening and softening behaviours, to better express UHPFRC properties.

In this study, the static test is performed to obtain the material properties for the numerical modelling, from the test pressure-deflection curve of UHPFRC specimen can be obtained.

In the test, the UHPFRC slab with dimension of 660 x 660 x 25 mm was tested by uniformly distributed loading in a pulse pressure loading rig, developed by University of Liverpool (Schleyer, et al. 2012), which is depicted in Figure 17.

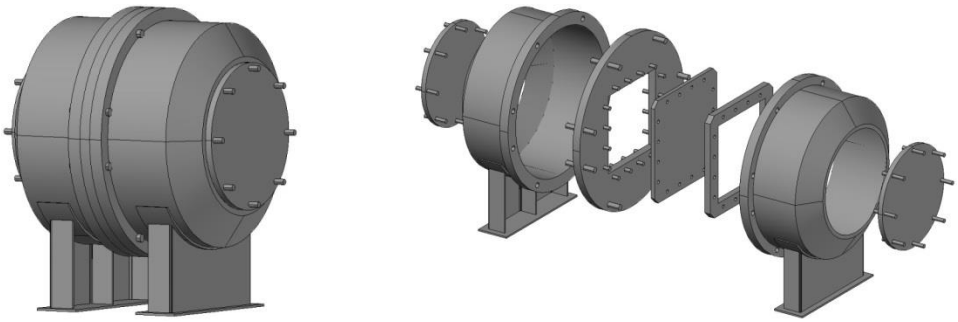

(a) Assembled view (b) Expanded view

Figure 17 Pulse pressure loading rig (PPLR) used in static mode

The UHPFRC specimen was mounted in the central section of the loading rig with a rubber strip used to provide an air tight around the edge of 500mm square loaded area. The central deflection of UHPFRC specimen was measured with a linear variable differential transformer (LVDT), and the pressure applied to UHPFRC specimen was measured using pressure gauges. In the test, one side of the rig was pressurised with air in stages and the specimen deflection was recorded at each loading step. Figure 18 shows the collected pressure-deflection curves from UHPFRC specimen with different fibre volumes. It can be seen that the failure of specimen cannot be controlled due to the means of loading, thus when the specimen ruptured abruptly when it was tested to failure, it was not possible to obtain the data in the strain-softening region for the complete pressure-deflection curve.

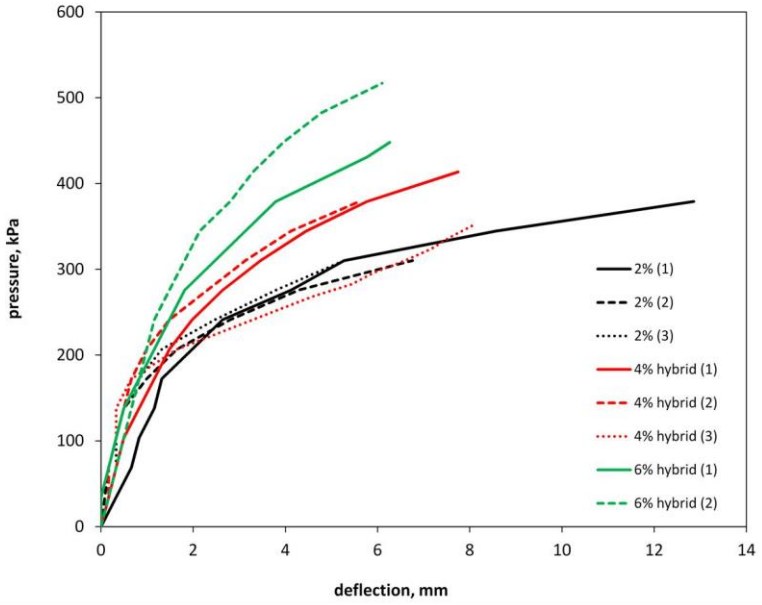

383

384 Figure 18 Pressure-deflection relationships for UHPFRC specimen obtained under static uniformly
385 distributed loading

386 Due to the fact that complete information about UHPFRC material properties cannot be
387 collected from the tests, the design stress-strain curve from UHPFRC with 2% fibre volume is
388 employed for the modification of generated model parameters, which is depicted in Figure
389 19, and Table 2 lists some key values of the design curve. Using this design curve, the
390 numerical model of UHPFRC beam with 2% fibre volume can be developed directly, model
391 parameters controlling strain hardening and softening are modified to let the modelled
392 stress-strain curve matches the design stress-strain relationship, while for UHPFRC beam
393 with 6% and 6% hybrid fibre volumes, as increased fibre volumes may not only change
394 compressive strength of UHPFRC, but also its stress-strain shape (Barnett et al. 2010), thus
395 the increased compressive strength and updated design stress-strain curve should be
396 applied to modify model parameters of UHPFRC beam model with 6% fibre volumes.

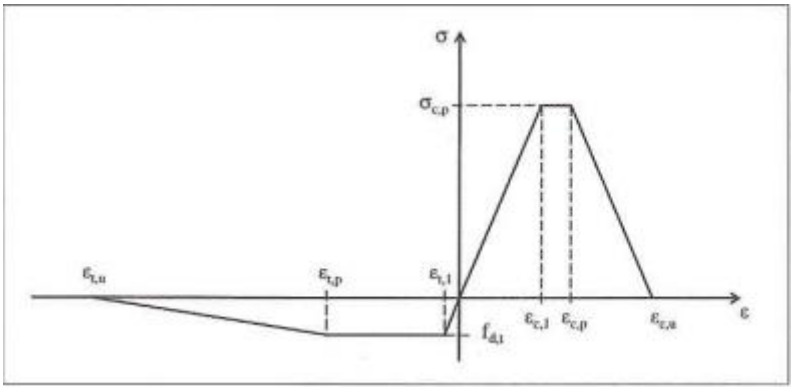

Figure 19 Design stress strain curve from UHPFRC with 2% fibre volume

Table 2 Material Properties of UHPFRC slab

Tension		Compression	
Tensile strength ($f_{d,t}$) with 2% fibre volume	10MPa	Compressive strength ($\sigma_{c,p}$) with 2% fibre volume	170MPa
Tensile strength ($f_{d,t}$) with 6% fibre volume	15MPa	Compressive strength ($\sigma_{c,p}$) with 6% fibre volume	200MPa
Max linear strain ($\varepsilon_{t,l}$)	0.00011	Max linear strain ($\varepsilon_{c,l}$)	0.0031
Limiting tensile strain ($\varepsilon_{t,p}$)	0.004	Limiting compressive strain ($\varepsilon_{c,p}$)	0.004
Max tensile strain ($\varepsilon_{t,u}$)	0.01	Max compressive strain ($\varepsilon_{c,u}$)	0.007

401 According to previous study (Mao, et al. 2014), the variation of DIF value with strain rate
402 under compression and tension can be expressed as:

403 $$\text{Compression } DIF = \begin{cases} \left(\frac{\dot{\varepsilon}}{\dot{\varepsilon}_s}\right)^{1.026\alpha} & \dot{\varepsilon} \ll \dot{\varepsilon}_1 \\ A_1 \ln(\dot{\varepsilon}) - A_2 & \dot{\varepsilon} > \dot{\varepsilon}_1 \end{cases} \quad (1)$$

404 where $\dot{\varepsilon}$ is strain rate, $\dot{\varepsilon}_s = 3 \times 10^{-5} s^{-1}$ is the quasi-static strain rate, $\alpha = 1/(20 + f_{cs}/2)$,
405 f_{cs} is the static compressive strength, $\dot{\varepsilon}_1 = 0.0022 f_{cs}^2 - 0.1989 f_{cs} + 46.437$ ($\dot{\varepsilon}_1$is 79s^{-1} in
406 this case), $A_1 = -0.0044 f_{cs} + 0.9866$, $A_2 = -0.0128 f_{cs} + 2.1396$.

407 $$\text{Tension } DIF = \begin{cases} \left(\frac{\dot{\varepsilon}}{\dot{\varepsilon}_s}\right)^{\delta} & \dot{\varepsilon} \ll 30 s^{-1} \\ \beta \left(\frac{\dot{\varepsilon}}{\dot{\varepsilon}_s}\right)^{1/3} & \dot{\varepsilon} > 30 s^{-1} \end{cases} \quad (2)$$

408 where $\dot{\varepsilon}_s = 10^{-6} s^{-1}$, $log\beta = 7.11\delta - 2.33$, $\delta = 1/(10 + 6\, f_{cs}/f_{co})$, f_{cs} is the static
409 concrete compressive strength, $f_{co} = 10MPa$.

410 Several simplifications were made in the study to reduce the complexity of UHPFRC model
411 without affecting final results (Mao, et al. 2014). Steel fibres are not modelled explicitly, and
412 its effect is achieved by matching the modelled stress-strain curve from homogeneous
413 model to design stress-strain relationship of UHPFRC. Moreover, in the model, the supports
414 are not simulated, and the UHPFRC beam is simply supported by constraining vertical
415 displacement of supported area. It should be mentioned that in the numerical study, only
416 UHPFRC beams with 2% and 6% fibre volumes were investigated due to limited information
417 from UHPFRC specimen with 6% hybrid fibre volume.

418 It should be mentioned that the performance of K&C model in predicting UHPFRC behaviour
419 under blast loading have been studied in some previous researches (Mao, et al. 2014, 2015),

where both the deflection and failure mode of UHPFRC specimen can be predicted with good quality.

Figure 20 depicts the developed UHPFRC beam model, the drop hammer is modelled as sphere shape using *MAT_ELASTIC model, which can give same contact area as in the tests, and fibreboard is modelled with *MAT_PLASTIC_KINEMATIC model. Moreover, element size of beam model is selected as 2.5mm×2.5mm×2.5m after mesh convergence study.

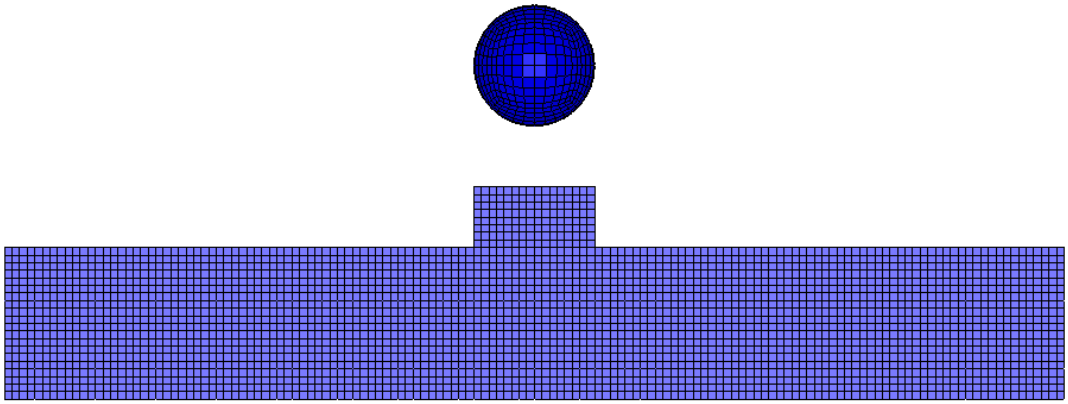

Figure 20 Developed UHPFRC beam model

3.2 Numerical investigation of support load

From section 2, it can be seen that the measured support load contain noisy spurs, and high-pass filter is applied to remove these spurs. In this section, the developed model will be employed to study the information in the support load, and extract natural frequencies of UHPFRC to evaluate its condition after the impact load.

Figure 21 depicts modelled support loads from beams with 2% and 6% fibre volumes (with 1m hammer releasing height). From the figure, spurs still appear in the support load. Moreover, more spurs can be found in the support load from beam with 6% fibre volume.

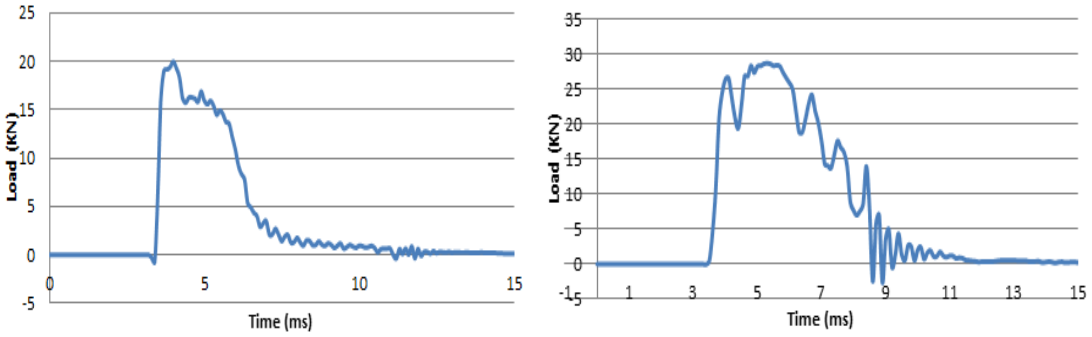

Figure 21 Support loads from developed beams with 2% fibre volume (left) and 6% fibre volume (right)

It can be seen from Figure 21 that before the impact load, a negative reaction force is appeared in the UHPFRC model with 2% fibre volume before the positive reaction force, this is due to the inertia effect which can give a value in opposite phase with impact load [Cotsovos, 2010, Kishi and Mikami, 2012]. However, it should be noted that this negative reaction force cannot be observed in UHPFRC model with 6% fibre volume, the reason is that the increase of fibre volume can improve the UHPFRC resistance to the impact load effectively, thus less inertia effect can be excited with the same impact load. Moreover, it can be seen that due to the inertia force in the UHPFRC model, the impact load will show several fluctuations after the peak load value. This can be used to confirm that the inertia effect is included in the developed UHPFRC model, and the model can be used to study the UHPFRC dynamic behaviour under impact loading condition effectively.

With the developed model, the first few natural frequencies from UHPFRC beam with 2% fibre volume are extracted, these frequencies are then compared to those from tested data, Figure 22 depicts the comparison results of power spectrum from whole support load and free vibration part after cutting support load. Similar frequency peak around 3000Hz can be

found in both curves, which confirms that the developed model can provide reliable the behaviour of UHPFRC beam under impact loading.

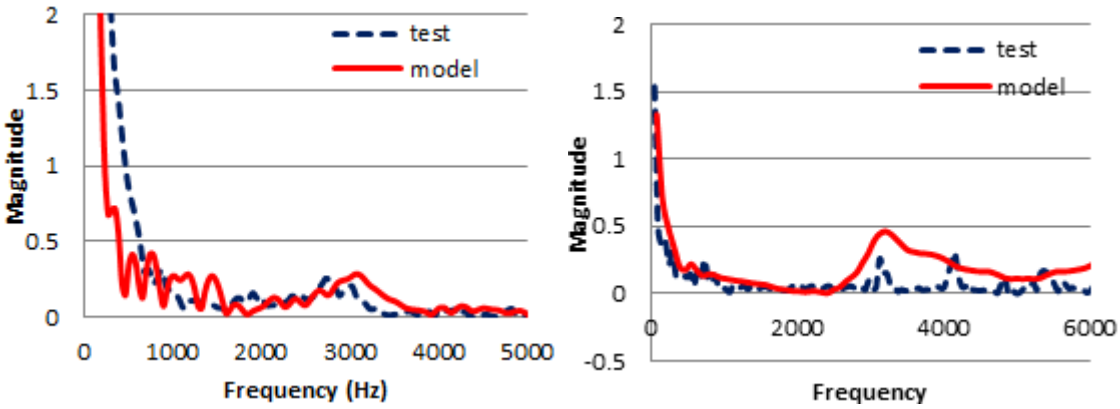

(a) Power spectrums of whole support load (b) Power spectrums of cutted support load

Figure 22Comparison of power spectrums from tested and modelled support loads

However, by comparing it with the natural frequencies of intact UHPFRC beam, which were obtained from developed model with modal analysis and listed in Table 3 (Table 3 also includes frequencies from power spectrum of tested support load of UHPFRC beam with 6% fibre volume), the 1st natural frequency of the UHPFRC beam cannot be found in Figure 22, the reason that in the above case, the beam is damaged completed after the impact loading. For further confirm the performance of developed model, the frequencies in the support load of with 0.5m impact hammer release height are extracted, where the UHPFRC beam with 6% fibre volume only experiences minor damage, the results are depicted in Figure 23. It can be seen that the 1st natural frequency at about 1300Hz can be observed clearly, which further validates the performance of the developed model.

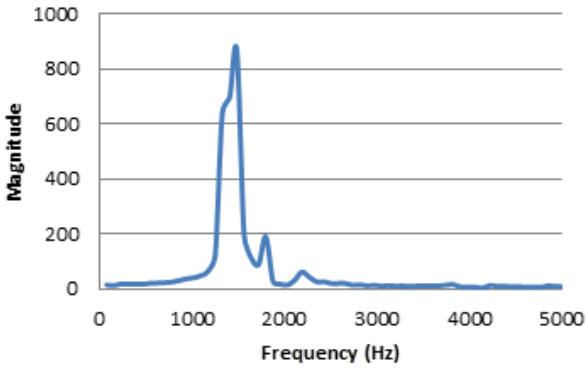

469

470 Figure 23 Power spectrum of support load from model at 0.5m high drop hammer

471 Table 3 Natural frequencies of UHPFRC beam

Mode	Modelled UHPFRC beam with 2% fibre volume	Modelled UHPFRC beam with 6% fibre volume	Tested UHPFRC beam with 6% fibre volume
1st bending mode	1237.9Hz	1284.9Hz	732Hz
1st torsion mode	3499.4Hz	3643Hz	3125Hz
2nd bending mode	4239.1Hz	4413.6Hz	4150Hz
2nd torsion mode	7019.2Hz	7309.5Hz	5422Hz

472

473 Moreover, from results in Table 3, it can be seen that from the tests, after the impact
474 loading, natural frequencies from the first few modes can still be extracted from UHPFRC
475 beam with 6% fibre volume, but compared to the numerical natural frequencies, significant
476 reduction can be observed. As the 1st natural frequency of beam can be calculated with the
477 following equation, the beam condition after impact load can be evaluated:

478 $$\omega_n = A\sqrt{EI/\mu L^4} \quad (3)$$

where A is the constant value and will be changed for different boundary conditions, E is Young's modulus, I is area moment of inertia, L is beam length, and μ is mass per unit beam length.

By comparing natural frequencies of beam before and after impact load, it can be estimated that after the impact load, rigidity (EI) of damaged beam is only 32% of its original value, this can be used to evaluate the damage level and the remaining strength of the beam.

3.3 Numerical results of UHPFRC beams with 2% fibre volume

As described in section 3.1, UHPFRC beam model with 2% fibre volume is developed and its stress-strain relationship is modified to match the design curve. It should be mentioned that the same procedure is used to obtain the relationship between strain rate and toughness, i.e. impact hammer is released to the UHPFRC beam, and load-deflection curve can be obtained. From the results, the toughness can be calculated using the area below the load-deflection curve, while strain rate is obtained by reading strain rate time-history from middle element on the beam bottom surface in LS-DYNA results.

In the model, various strain rates are obtained by releasing hammer from different heights, which is achieved by defining velocity of the drop hammer based on corresponding releasing height. From the results, the strain rate-toughness curve can be generated, which is depicted in Figure 24.

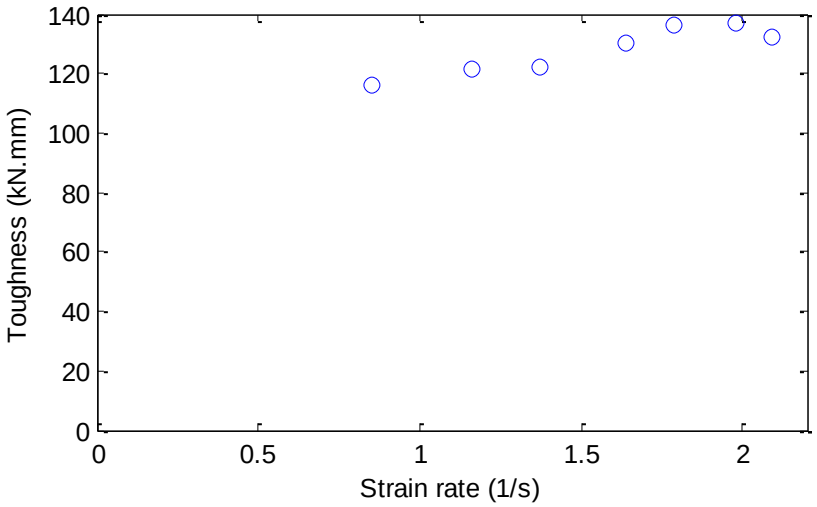

Figure 24 Relationship of strain rate and absorbed energy of UHPFRC beams with 2% fibre volume from model

From above results, it can be observed that the toughness of UHPFRC specimen will increase with strain rate. It should be noted that this increase trend is not clearly, thus it can be masked by the random effect of fibre orientation and distribution in the test results shown in section 2.

3.4 Numerical results of UHPFRC beams with 6% fibre volume

As mentioned in section 3.1, when modelling UHPFRC beam with 2% fibre volume, the design stress-strain curve (shown in Figure 19) can be used directly, as the design curve is from UHPFRC specimen with 2% fibre volume, while for UHPFRC beam with 6% fibre volume, the stress-strain curve should be changed due to increase of fibre volume, not only for concrete strength, but also for the shape of curve. In this study, without stress-strain curve from UHPFRC specimen with 6% fibre volume, the concrete compressive and tensile strengths are increased for UHPFRC beam with 6% fibre volume (listed in Table 2), and

model parameters controlling strain hardening and softening behaviours are modified to match the tested force-deflection curve from UHPFRC beam with 6% fibre volume.

Similar to UHPFRC beam cases with 2% fibre volume, beam toughness vs. strain rate relationship is obtained using developed UHPFRC beam model with 6% fibre volume using the same procedure. Figure 25 shows the relationship of beam toughness and strain rate from beam with 6% fibre volume.

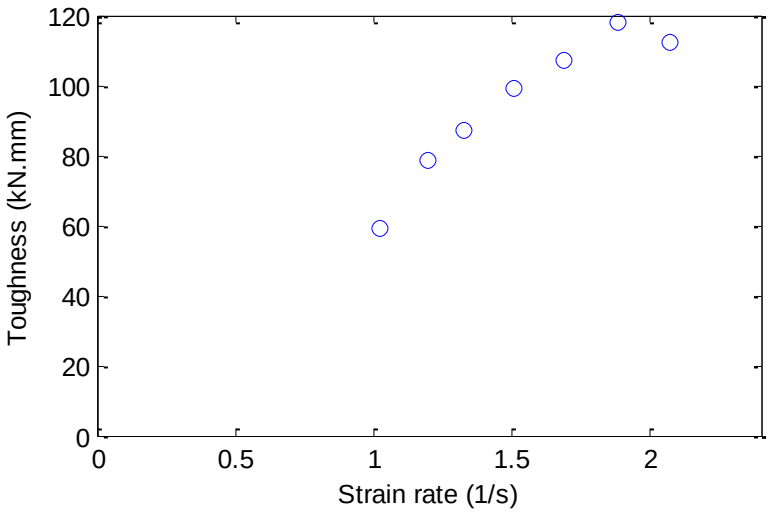

Figure 25 Relationship of strain rate and absorbed energy of UHPFRC beams with 6% fibre volume from model

From above figure clearly increase trend of toughness is observed, indicating increased fibre volume in UHPFRC specimen can give more significant strain rate effect. Moreover, UHPFRC specimen with 6% fibre volume shows improved resistance to impact load, this can be found that the starting strain rate is higher than $1s^{-1}$ in Fig.20, where the specimen has complete fracture, this value is larger than the strain rate leading to collapse of UHPFRC specimen with 2% fibre volume

Furthermore, the root mean square error (RMSE) is used to evaluate the toughness from the developed UHPFRC model, which can be calculated as follows, and results are listed in Table 4.

$$\mathrm{RMSE} = \sqrt{\frac{\sum_{i=1}^{n}(\hat{y}_i - y_i)^2}{n}} \quad (1)$$

Where n is the number of measurements (number of toughness values herein), y_i and y_i are the toughness values from the measurement and developed model at the same strain rate, respectively.

Table 4 Root mean square error between tested and simulated toughness-strain rate relationships

Fibre volume in UHPFRC specimen	Number of toughness values	RMSE
2%	13	20.07
6%	12	13.39

It can be seen from Table 4 that high RMSE values are observed, the reason is that in the test, the toughness value may show great variation even at the same strain rate, which is caused by the effect of random fibre orientation and distribution. With further increase of fibre volume in UHPFRC specimen, this random effect can be reduced effectively, and smaller RMSE value can be obtained for UHPFRC with 6% fibre volume. This further confirms the necessity of using numerical model for the better understanding of UHPFRC behaviour under high strain rate loads.

543 Moreover, the crack pattern of UHPFRC beam model with 6% fibre volume is shown in
544 Figure 26, where bending failure mode can be observed, and severe damage (cracks) are
545 located at mid-span of the UHPFRC beam, which is consistent to the results observed from
546 the tests (shown in Figure 11). This indicates the effectiveness of using UHPFRC model for
547 predicting UHPFRC behaviour and crack pattern under high strain rate loads.

548 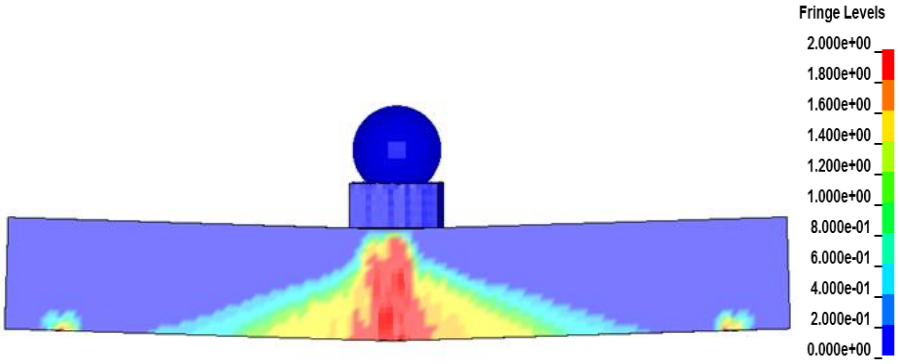

549 Figure 26 Damage of UHPFRC model with 6% fibre volume under impact loading

550 ## 4. Conclusions

551 In this paper, and the evolution of UHPFRC beam toughness with strain rate is investigated
552 using both experimental and numerical studies. UHPFRC beams with various fibre volumes
553 are employed for the analysis. In the experimental tests, various hammer release heights
554 and fibreboard layers are employed to get a set of strain rates.

555 With test data, UHPFRC beam toughness and corresponding strain rate can be obtained.
556 From the results, the increase of UHPFRC (with 2% fibre volume) toughness with strain rate
557 cannot be observed clearly.

558 With increased fibre volume in UHPFRC specimen, the toughness increase trend with strain
559 rate can be observed, and the blast resistance of UHPFRC specimen is also increased.

560 Moreover, the effect of fibre with different lengths is studied, results demonstrate that the
561 UHPFRC beam with fibre combination can only give slight higher toughness, especially at
562 high strain rate range.

563 Considering the influence of random fibre orientation and distribution is not considered in
564 the tests, numerical analysis is performed in LS-DYNA to further study the beam toughness
565 with increased strain rate. A UHPFRC beam model is developed and its performance under
566 impact load is validated, in the model, the parameters controlling strain hardening and
567 softening behaviours are modified to match stress-strain relationship from UHPFRC
568 specimen. Results show increased UHPFRC toughness with strain rate from specimen with
569 both 2% and 6% fibre volumes, while UHPFRC specimen with high fibre volume will give
570 more clearly toughness increase trend, and strain rate effect and blast resistance are
571 improved with increase of fibre volume in UHPFRC specimen.

572 Acknowledgements

573 The authors are grateful to the Faculty of Technology and School of Civil Engineering and
574 Surveying at the University of Portsmouth for financial support. The test data described
575 here was collected as part of an EPSRC-funded project at the University of Liverpool. The
576 authors gratefully acknowledge the significant contributions to this work by Professor Steve
577 Millard (formerly University of Liverpool), Bekaert, VSL Australia, CPNI and GL Industrial
578 Services.

579 Reference

580 Barnett, S.J. Development of advanced concrete materials for anti-terrorism applications.
581 The Structural Engineer, October 7, 2008, 28-29.

582 Barnett, S.J., Lataste, J.F., Parry, T., Millard, S.G., Soutsos, M.N. Assessment of fibre
583 orientation in ultra high performance fibre reinforced concrete and its effect on flexural
584 strength. Materials and Structures, 2010, 43(7): 1009-1023.

585 Bragov, A.M., Petrov, Y.V., Karihaloo, B.L., Konstantinov, A.Y., Lamzin, D.A., Lomunov, A.K.,
586 Smirnov, I.V. Dynamic strengths and toughness of an ultra high performance fibre reinforced
587 concrete. Engineering Fracture Mechanics, 2013, 110, 477-488.

588 Cotsovos, D.M. A simplified approach for assessing the load-carrying capacity of reinforced
589 concrete beams under concentrated load applied at high rates. International Journal of
590 Impact Engineering, 2010, 37(8), 907-917.

591 Habel, K., Viviani, M., Denarie, E., Bruhwiler, E. Development of the mechanical properties
592 of an ultra-high performance fiber reinforced concrete (UHPFRC). Cement and Concrete
593 Research, 2006, 36(7), 1362-1370.

594 Isaacs, J., Magallanes, J., Rebentrost, M., Wight, G. Exploratory dynamic material
595 characterizing tests on ultra-high performance fiber reinforced concrete. 8th International
596 Conference on Shock & Impact loads on structures, December 2-4, 2009, Adelaide, Australia.

597 Kang, S.T., Lee, Y., Park, Y.D., Kim, J.K. Tensile fracture properties of an ultra high
598 performance fiber reinforced concrete (UHPFRC) with steel fiber. Composite Structures,
599 2010, 92(1), 61-71.

600 Kim, D.J., Park, S.H., Ryu, G.S., Koh, K.T. Comparative flexural behaviour of hybrid ultra high
601 performance fiber reinforced concrete with different macro fibers. Construction and
602 Building Materials, 2011, 25(11), 4144-4155.

603 Kishi, N., Mikami, H. Empirical formulas for designing reinforced concrete beams under
604 impact loading. ACI Structural Journal, 2012, 109(4), 509-520.

605 Magallanes, J.M., Wu, Y., Malvar, L.J., Crawford, J.E. Recent improvement to release III of
606 the K&C concrete model, June 6-8, 2010, Dearborn, Michigan, USA.

607 Malvar, L.J., Crawford, J.E., Wesevich, J.W., Simons, D. A plasticity concrete material model
608 for DYNA3D. International Journal of Impact Engineering, 1998, (9-10), 847-873.

609 Malvar, L.J., Crawford, J.E., Morrill, K.B. K&C concrete material model release III –
610 automated generation of material model input. K&C Technical Report TR-99-24-B1,
611 Glendale, CA, 2000.

612 Mao, L., Barnett, S.J., Begg, D., Schleyer, G.K., Wight, G. Numerical simulation of ultra high
613 performance fibre reinforced concrete panel subjected to blast loading. Journal of cement
614 and concrete composites, 2014, 64: 91-100.

615 Mao, L., Barnett, S.J., Tyas, A., Warren, J., Schleyer, G.K., Zaini, S.S. Response of small scale
616 ultra high performance fibre reinforced concrete slabs to blast loading. Construction and
617 Building Materials, 2015, 93: 822-830.

618 Millard, S.G., Molyneaux, T.C.K., Barnett, S.J., Gao, X. Dynamic enhancement of blast-
619 resistant ultra high performance fibre-reinforced concrete under flexural and shear loading.
620 International Journal of Impact Engineering, 2010, 37(4), 405-413.

621 Mechtcherine, V., Silva, F.A., Butler, M., Zhu, D., Mobasher, B., Gao, S.L., Mader, E.
622 Behaviour of strain-hardening cement-based composites under high strain rates. Journal of
623 Advanced Concrete Technology, 2011, 9(1), 51-62.

624 Naaman, A.E., Reinhardt, H.W. High performance fibre reinforced cement composites 2
625 (HPFRCC2). Proceedings of the 2nd International Workshop 'High Performance Fibre
626 Reinforced Cement Composites', Ann Arbor, USA, 1995.

627 Odeh, A.A. Modelling and Simulation of bogie impacts on concrete bridge rails using LS-
628 DYNA. 10th International LS-DYNA Users Conference, Dearborn, Michigan, USA, 2008.

629 Park, S.H., Kim, D.J., Ryu, G.S., Koh, K.T. Tensile behaviour of ultra high performance hybrid
630 fiber reinforced concrete. Cement and Concrete Composites, 2012, 34(2), 172-184.

631 Schleyer, G.K., Underwook, N.J., Do, H.M., Paik, J.K., Kim, B.J. On pulse pressure loading of
632 plates with holes, Central European Journal of Engineering, 2012, 2(4), 496-508.

633 Schleyer, G.K., Barnett, S.J., Millard, S.G., Wight, G. Modelling the response of UHPFRC
634 panels to explosive loading. 11th International Conference on Structures under Shock and
635 Impact, Tallinn, Estonia, 2010.

636 Tanapornraweekit, G., Haritos, N, Mendis, P., Ngo, T. Modelling of a reinforced concrete
637 panel subjected to blast load by explicit non-linear FE code. Proceedings of Earthquake
638 Engineering in Australia Conference 2007, Wollongong, NSW, Australia, 2007.

639 Tu, Z.G., Lu, Y. Evaluation of typical concrete material models used in hydrocodes for high
640 dynamic response simulations. International Journal of Impact Engineering, 2009, 36(1),
641 132-146.

642 Yi, N.H., Kim, J.H.J., Han, T.S., Cho, Y.G., Lee, J.H. Blast-resistant characteristics of ultra-high
643 strength concrete and reactive powder concrete. Construction and Building Materials, 2012,
644 28(1), 694-707.